Rice University 2023–2024 Turbine Design Report

President
Raj Anthony

Vice President and Treasurer
Maya Chhong

Mechanical Team
Izzie Driewer, Esther Fahel
Ethan Goore, Adeel Sumar
Caesar Coss, Jasmine Klinkao
Megan Worstell, Rachel Kim
Amelia Pillar, Brian Mercado
Sherry Choi, Kenton Roberts

Electrical Team
James Mahoney, Raj Anthony
Elliot Chae, Adam Swartz
Alessandro Bordone, Jason Yang

Pitch System Contributors
Bryce Kim, Brianna Schulstad
Mert Culcu, Peter Humphreys
Noemi Moreno, Aidan McKenna
Summer Barrette, Jorge Quintero
Remy Hurtado

Consulted Mentors
Dr. David Trevas (Faculty Advisor)
Dr. Gary Woods, Joe Gesenhues

Sponsors
US Department of Energy
Oshman Engineering Design Kitchen
Rice Engineering Alumni
RWE

Team Contact Information
ricewindclub@gmail.com

Table of Contents

1.0 Executive Summary

Rice Wind Energy endeavored to optimize a small-scale wind turbine to compete in the testing categories for turbine design set by the 2024 Collegiate Wind Competition in power performance, controllability, safety, and durability. To work towards our goal, Rice Wind Energy branched off into two subteams: Mechanical and Electrical. We also sponsored freshman and senior design projects focused on aiding with pitch system development.

The Mechanical team presided over the foundation, base plate, tower, nacelle housing, pitch system, and blades. To anchor our offshore turbine in the tank, we created a suction caisson foundation that uses the creation of negative pressure between the base of the bucket and the sand to oppose movement. The base plate and tower are made from 6061 aluminum and TIG welded at the base. The nacelle is 3D printed from PLA and sits on a brass sleeve bearing which provides yaw capability. We built a mechanical disc brake system to slow the shaft alongside our pitch system. The blades were made with Schmitz optimization equations and simulated in QBlade software. Evaluated against 14 airfoils, we chose the SD7003-085-88 airfoil for its high and broad power curve. We chose to SLA print our blades from FormLabs Tough 1500 resin for its demonstrated strength in tension and its smooth finish.

The freshman design project created our initial pitch system prototype, which was improved by the Mechanical team. Our pitch system rotates the blades between 0 and 100 degrees using a linear actuator. This allows us to meet the tasks of power curve performance and controllability. During emergency stop and the durability task, the pitch system feathers the blades completely out of the wind. The senior design pitch project contributed power optimization and controllability code and logic.

The Electrical subteam built the system that enables our turbine to adapt to varying wind speed conditions in order to maximize power output. An anemometer is employed to gather wind speed data and a hall effect sensor is employed to capture the generator's RPM. This data is then processed by software on an Arduino which produces control signals to various subsystems, such as the linear actuators that control the pitch of the turbine's blades, or the MOSFET switches that connect and disconnect our generator from our variable load. When the load is disconnected or the emergency stop button is pushed, a charged capacitor will power the linear actuators to activate the brake disc and pitch the blades out of the wind. This control through the electrical system is crucial, and results in the versatile and safe operation of our wind turbine. The final turbine CAD and assembly are shown in Figure 1 below.

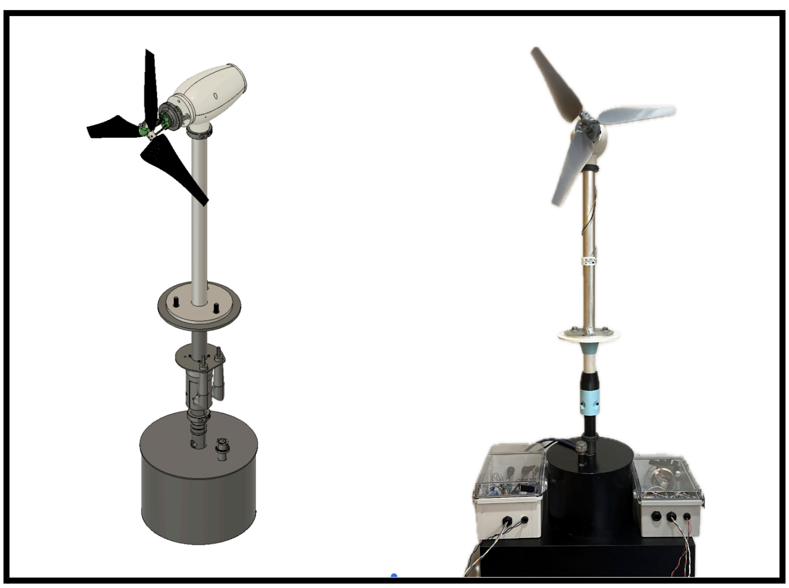

Figure 1: Full Turbine Assembly CAD and Final Prototype

2.1 Design Objective

The objective of our project is to design and manufacture an aerodynamic, durable wind turbine that can optimize power production, output a stable power reading when necessary, and be able to shut off quickly in emergencies. The turbine must be in accordance with the CWC constraints and safety requirements.

Our turbine should know which turbine testing task it is completing and react accordingly. We implemented code via an Arduino IDE that identifies RPM and wind speed bins from our optically isolated hall effect sensor and anemometer outputs. Between 5-11 m/s, the turbine should optimize power production and between 12-14 m/s, it should maintain the same power output and RPM as at 11 m/s. We designed and optimized our blades to capture as much energy from the wind as possible, and built a pitch system to assist with startup and modulate RPM as necessary. This is done with code that continuously records RPM and wind speed to identify the optimal pitch for maximum power generation.

The turbine must detect emergency stop or loss of power and reach 10% of its operational RPM within 10 seconds. We have an Arduino pin that simulates a voltmeter to recognize a sudden drop of power generation when the PCC is broken. Then, corresponding code activates the pitch system and mechanical brake.

Our turbine should endure fluctuating wind speeds of up to 22 m/s without any component failures, while remaining upright on our foundation. We will use our disc brake and pitch system to ensure the shaft does not rotate to avoid component failure and reduce drag force in high wind speeds. In addition, we have ensured adjustability of our foundation top tube to meet installation requirements and created a simple foundation design out of a lightweight-gauge sheet metal.

In prioritizing quick commissioning time and electrical safety, our electrical system has been placed in non-metallic circuit enclosures (one for the turbine side circuitry and one for load side circuitry). They have no sharp edges and pose no safety risks. We have ensured that no wires inside our system are loose. The wires are routed through cable glands in the sides of the boxes to protect against strain and chafe on the cables. Furthermore, the wires coming into and out of each box (nacelle to turbine side box, and turbine side box to load side box) are fastened with secure connectors that make transportation and commissioning of our system straightforward. We have selected a generator that will not surpass the 48 Volt limit within the RPM range our turbine will be tested at, as well as RPMs slightly above this range, so we do not anticipate a risk of overloading our system with voltage or power.

2.2 Similarities in the Design

Rice Wind Energy brought a turbine to the competition as a learn along team last year. Similarities and changes from that turbine are described below, followed by ways in which the winning teams (Johns Hopkins and Kansas State) influenced our design since we did not compete.

2.2.1 Similarities with Last Year's Design

Nacelle: The strategy of creating custom component supports and printing out of PLA was adopted again to allow for precise component alignment and fast manufacturing turnaround time.

Brake: Instead of pressing a dremel pad against an acrylic disc attached to our main shaft to mechanically brake, we use a linear actuator which closes RC car disc brake calipers, chosen for their strong contact friction.

RPM Measurement: Like last year's turbine, this year we are using a Hall effect sensor to measure RPM because of its simplicity. However, the magnet, orientation and placement, and code used to calculate RPM have all been changed and improved this year.

Microcontroller: We are also using the same model of microcontroller compared to last year: an Arduino Uno R3. This is due to its wide variety of GPIO pins and strong community, which allow us to utilize a diverse set of libraries and write quicker and more effective code.

Electrical Enclosure: We are utilizing the same box for our turbine-side circuitry because it secures the components in accordance with NEMA 1 standards and provides a safe and reliable way to store our circuit.

2.2.1 Similarities with Winning Reports

Pitch: We implemented a pitch system for the first time this year. The system includes the same main components as RC helicopter pitch systems while featuring curved legs like those seen on Kansas State's turbine. The curves allow for a larger pitch angle threshold without components rubbing

Brake: After deciding to use a disc brake this year, we were inspired by Johns Hopkins' small RC disc brake calipers. We bought different ones of similar size, and actuate with a linear actuator instead of Johns Hopkins' method of using a wire.

Foundation: Our foundation is similar to the suction bucket used by Johns Hopkins. However, we install and seal the foundation in a different way. We also have an adjustability system in our foundation that is not seen in any other team.

Generator: Our choice of the Nanotec DB42C01 brushless DC motor as our generator was influenced by the one utilized by Kansas State in their successful turbine design. The motor greatly improves efficiency and power output compared to our brushed DC motor last year. Further, we built a three phase rectifier following the motor that converts the three phase output to a smooth DC to provide power to the load and necessary circuit components.

2.3 Blades and Static Performance Analysis

2.3.1 Blade Design

This year, our intent was to design our three-blade rotor to maximize power output in 5-11 m/s wind. To understand the parameters and theory behind blade design, we read *Wind Energy Explained: Theory, Design, and Application* by J. F. Manwell, and watched Dr. Nordenholz' YouTube series on OpenEI. We first chose our rotor optimization method and then applied it to many airfoils to analyze their differences.

To determine the chord and twist of our blades, we chose the following Schmitz optimization equations from Chapter 3.9 of *Wind Energy Explained* for their observation of wake rotation.

$$\phi = \frac{2}{3} tan^{-1}\left(\frac{R}{\lambda r}\right) \qquad \theta_p = \phi - \alpha \qquad c = \frac{8\pi r}{BC_L}(1 - cos(\phi))$$

In the following equations, ϕ is the angle of the approaching relative wind speed, R is the total blade length, r is the local radial position, θ_p is pitch angle, α is optimal angle of attack, c is chord, B is number of blades, and C_L is coefficient of lift. We began by approximating the optimal tip speed ratio as $\lambda_{opt} \approx \frac{4\pi}{B} = \frac{4\pi}{3} \approx 4.2$ [1]. We ran a polar analysis on QBlade software's integrated XFoil program, at our expected Reynolds number (Re) of 50,000. This enabled us to find our α at the highest coefficient of lift to coefficient of drag, as well as C_L at that optimum α for the Schmitz equations. We used our calculated chord and ϕ to create a rotor in QBlade V.0963. We were then able to simulate competition conditions on the rotor, accounting for Prandtl tip and root losses since we did not create wing tips to break vortices that would form. We verified that the Re and α were close to our input values in the latter half of the blade because that half generates more power. We also verified that the axial and tangential induction factors were around ⅓ and zero respectively for optimal performance.

After completing an initial test optimization, we repeated the above method on 14 airfoils with a thickness of no more than 10% from the Selig-Donovan series for their focus on low Reynolds number conditions. Our final step was creating a Cp vs λ power curve. Last year, our team assumed that the airfoil with the highest C_L/C_D would have the best power curve. This assumption was disproved in our analyses, which is why we created power curves for all 14 airfoils before comparing them. Our final choice, SD7003-085-88, had the highest and broadest peak, which guarantees excellent performance and gives us a large range of RPM values to operate in while producing lots of power.

Many teams deviate from 4.2 for their TSR, so we created rotors with several different TSRs around 4.2 to see how changing the TSR would impact the Cp vs λ graph. We created rotors with TSRs of 2, 3, 3.5, 3.8, 4, 4.2, 4.3, 4.5, 4.6, 4.7, 4.8, 4.9, 5, and 6, then analyzed the Cp vs λ graphs to find the rotors with the highest broadest peak. Power curves below TSR of 4.2 saw the peak begin to narrow, but all curves between 4.2 and 5 had high and broad peaks. Increasing TSR did not show an increase in Cp. Thus, we chose a TSR of 4.2 so our optimal RPM range would be lower and exert less stress on the blades, hub, and shaft. In addition, a lower TSR would allow us to create more torque at lower wind speeds.

We added a secondary airfoil, S8055, for structural stability near the root of the blade. This airfoil was chosen for its larger thickness (12%) and its relative geometric similarities to the SD7003-085-88. Three separate blends of airfoils were incorporated between the base and main airfoils to make the transition gradual and keep a smooth aerodynamic profile while still gaining the benefits of each airfoil where they perform best. The final Cp vs λ graph can be seen in Figure 2 below.

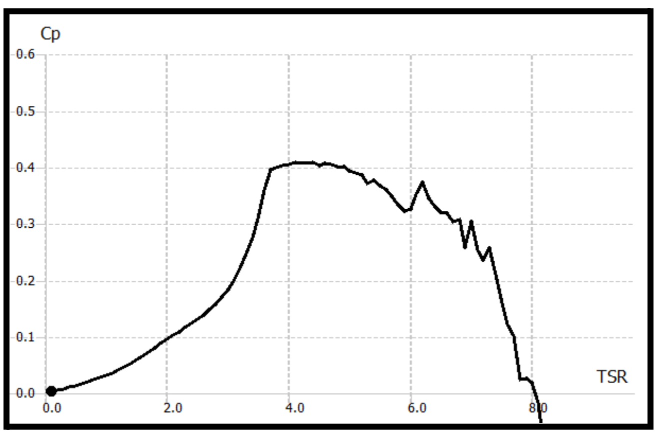

Figure 2: Cp vs λ Graph for Rotor with SD7003-085-88 and S8055 airfoils

2.3.2 Blade Static Performance Analysis

After we selected our final rotor, we input the dimensions and parameters of our blades into a self-designed Excel spreadsheet to extract several theoretical values to compare our physical testing with. We used formulations from *Wind Energy Explained: Theory, Design, and Application* to calculate radial and centripetal accelerations, flapwise and centripetal forces on the blades, maximum stresses, and blade deflections. It is important to note that the deflections only account for flapwise forces acting perpendicular to the face of the blades, not the centripetal forces. Thus, our deflection results are larger than they should be when testing, which is desired when designing for a higher factor of safety.

As this spreadsheet was a new addition this year, we decided to use it on multiple airfoils to get a sense of the scale of our numbers and rule out potential choices for our final blade. We were more confident in the formulations used to get our theoretical parameters in the Tensile Testing section of the report, so the values of our spreadsheet still have room for improvement and the inclusion of more important parameters. Next year we aim for this spreadsheet to be our primary method of obtaining our theoretical parameters.

From our wind tunnel testing described in section 2.11.1, we are able to produce a rated power of 9.46 Watts at 11 m/s. Assuming 8760 operational hours in one year and a projected capacity factor of 47% [2], our turbine design is able to attain an Annual Energy Production (AEP) of 38.95 kWh.

2.4 Engineering Diagram of Mechanical Systems and Analysis of Loads

2.4.1 Engineering Diagrams of Mechanical Systems

Nacelle and Yaw

The nacelle was designed around the components inside of it. These components include the generator, two linear actuators, two main bearings, a shaft coupling, and a disc brake and caliper. The nacelle was designed using Fusion360 CAD software to interface seamlessly with each component. The linear actuators and the motor are set in the bottom bed, pressed down by a lid with corresponding geometry to secure components. Through many iterations, we minimized the size of the nacelle to increase aerodynamics while keeping the structure strong. The linear actuator on the left of the generator is used to actuate the active pitch system described in the next section. The linear actuator to the right of the generator is used to press the sides of the brake calipers together around a disc for emergency braking. The caliper and linear actuator are interfaced with a 3D-printed transition piece. The disc brake is held in the correct position by a smaller shaft collar on either side. The main shaft is connected to the motor shaft with a flexible shaft coupling used to dampen vibrations in the system. The shaft is supported by two main bearings at the front of the nacelle. The lid is held in place by overlapping geometry with the bottom. To secure it further, heat set inserts are placed in two holes beside the linear actuators, and the lid screws into those. The faceplate keeps the main bearings in place. We chose to implement a stack of two main bearings, with a spacer in between, to cut down on the misalignment we encountered when just using one bearing.

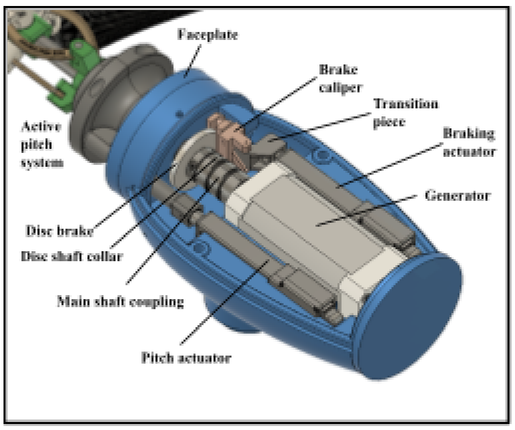

Figure 3: Nacelle Components

Pitch

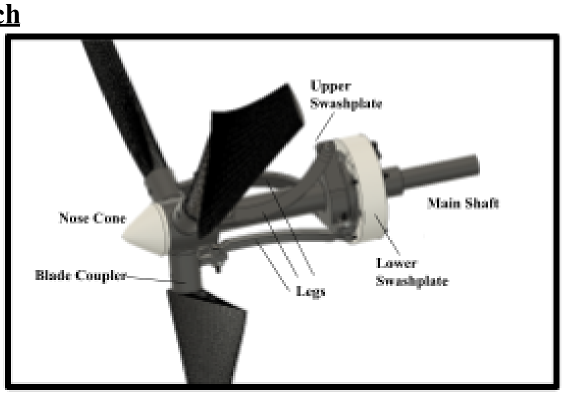

Figure 4: First Iteration Pitch System by Fall Design Team

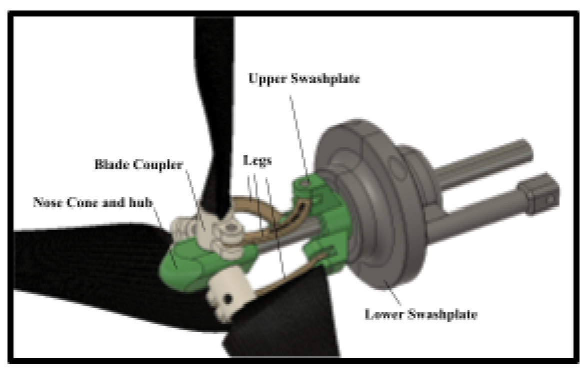

Figure 5: Spring Pitch System Redesign

This is the first year Rice Wind Energy is implementing an active pitch system. We worked with a freshman design team in the fall semester to design the basic components of the system. We took what they learned for a complete redesign early in the spring semester. Both active pitch systems work in fundamentally the same way. There are three legs connected, on one side, to couplers for the blades and an upper swashplate on the other side of the legs. The upper swashplate rotates along with the shaft and is connected to a stationary lower swashplate. This moves back and forth along the shaft resulting in the pitch of the blades.

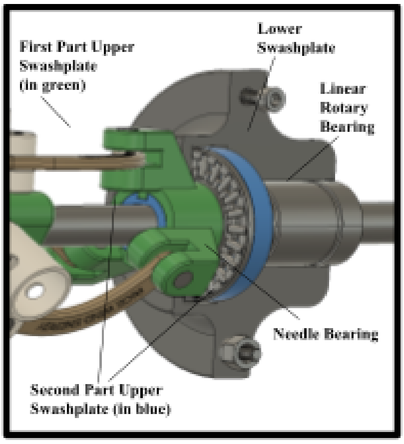

Figure 6: Section View of Swashplate Assembly

The first system required two linear actuators to move the lower swashplate. In the spring, we transitioned to using one linear actuator along with a linear-rotary bearing in the swashplate to mitigate the torque in the system from the one actuator. Two needle bearings were also added to take care of friction between the two swashplates. The upper swashplate consists of two pieces in order for the top needle bearing to be installed. The pieces lock together with a keyed shaft configuration and are then secured with two-part epoxy.

Other improvements included switching screws and locking nuts for a more permanent solution of brass pins. The brass pins sit flush in the design and allow for more range of motion with less weight. Another difference in the pitching systems comes from how the blade couplers interface with the main shaft. In the first design, more screws and locking nuts were used, but these had the tendency to unscrew during testing and were difficult to install. In the spring redesign, we incorporated shoulder screws which screwed directly into the shaft which we drilled and tapped. This eliminated the need for three nuts and significantly reduced our hub size. We also added small needle bearings in between the couplers and the hub to cut down on friction between the parts. The nosecone of the second pitch system is also sturdier. Instead of having to screw on a separate piece, the hub and nose cone are resin printed as one piece.

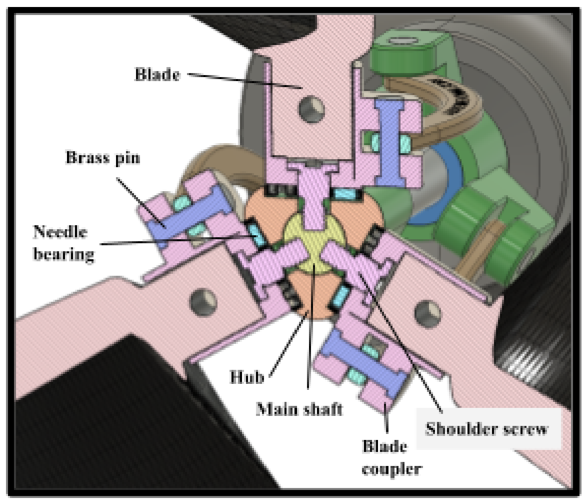

Figure 7: Section View of Hub Assembly

<u>Tower and Base plate</u>

The tower is constructed from a 1.5” diameter 6061 aluminum pipe. It features an offset section at the top in order to mount a brass sleeve bearing flush with the aluminum. This sleeve bearing gives our nacelle the ability to yaw, which is locked with a shaft collar during wind tunnel testing. The base plate was cut on a water jet to the competition specifications and then cleaned up using a lathe. The tower and base plate were TIG welded together by ACME Brass and Aluminum Manufacturing in Houston, TX. To incorporate an Earth-ground, we drilled and tapped a small hole in the top of the tower. The Earth-ground wire is screwed into this hole on the inside of the tower.

2.4.2 Tensile Testing

Blades were determined as a critical failure component due to their thin material and the high force fluctuations they undergo. Axial stress caused by the centripetal force during rotation was of primary concern, as were stress concentrations at the root of the blades due to the sudden change in geometry and small diameter. Testing our blade material’s tensile strength was imperative.

Our design space’s technicians recommended FormLabs Tough 1500 resin, so we decided to test that versus conventional PLA. We tensile tested identical coupons of each blade material and found that Tough 1500 resin was able to withstand time under tension for 14 mins and stretch 5.1 cm before failure. By comparison, the PLA only endured for 1.5 mins and stretched 0.4 cm before failure. This demonstrated Tough 1500’s superior elasticity, an important property for our blades to have to resist bending, and it's far superior tensile endurance. Additionally, the resin did not break along layer lines as the SLA printing process creates homogeneous pieces. Our tests determined that Tough 1500 resin has an ultimate tensile strength (S_{UT}) is 4839 psi. This aligns with the values on the FormLabs website. It is necessary to know what axial stress values are expected so we can determine the factor of safety. To do this requires calculations,

$$F_c = mr\omega^2 \qquad\qquad \sigma_{axial} = \frac{F_c}{A_{x-section}}$$

where F_c is the centripetal force, m is the mass of each blade, r is the blade length, ω is the angular velocity in radians per second, σ_{axial} is the axial stress, and $A_{x-section}$ is the cross-sectional area of the blade root. The maximum angular speed we expect to experience is 3000 RPM. This corresponds to a ω value of 31.416 radians per second.

$$F_c = 769.7\ \text{lb}_f, \qquad \sigma_{axial} = 3921\ \text{psi}, \qquad S_{UT} = 4786\ \text{psi}$$

This leads to a factor of safety of 1.23. While this is relatively low, 3000 RPM is a significant overestimate of the speeds our turbine is likely to experience.

2.4.3 Vibrational Testing

To avoid stress caused by resonant frequencies, it is important to understand what the resonant frequencies of the design are. We have done this in three ways: finite element analysis (FEA) modeling, physical modal analysis, and wind tunnel testing (see section 2.11.3).

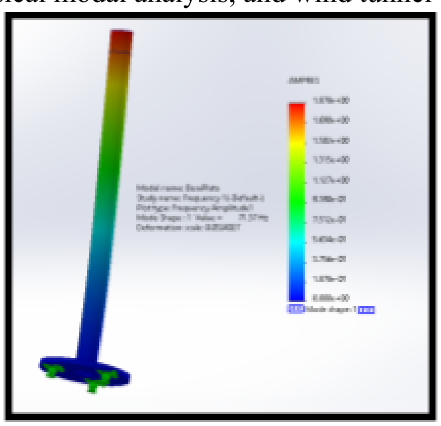

Figure 8: FEA of Baseplate and Tower

Using the FEA simulation feature in SOLIDWORKS, we conducted a frequency analysis simulation of our tower by applying fixed support boundary conditions on the three bolt holes and a point load to the end of the tower. Meshing the model and running the simulation gave a resonant frequency of 71.37 Hz which is equivalent to 4282.2 RPM. While there were additional frequencies corresponding to higher mode shapes, these frequencies would be excited by RPM values much higher than anything we would expect to experience.

FEA results do not take into account frictional damping forces, fixture strength, nacelle weight, blade stiffness, and numerous other factors that can affect resonant frequency. To more accurately determine the resonant frequencies of our turbine, we mounted an accelerometer on the top of the tower and struck the tower at various points from top to bottom using an impact hammer in a process known as modal analysis. The impact hammer measures the input force, and the accelerometer records the amplitude and frequency of vibration. Through these tests, we were able to produce frequency response functions showing the magnitude of vibration as a function of excitation frequency. In the vibration testing graphs, there was a single significant peak at 60hz. This corresponds to 3600 RPM and is above any RPM value we would expect to see.

2.5 Engineering Diagram of Foundation and Structural Analysis

Our foundation design is a caisson which stabilizes the tower by creating suction that resists movement when closed inside the sand. The design, shown in Figure 9 below, features the caisson covered with a top plate with its sole opening through a pipe nipple. The nipple is sealed by a pipe cap to create the suction chamber.

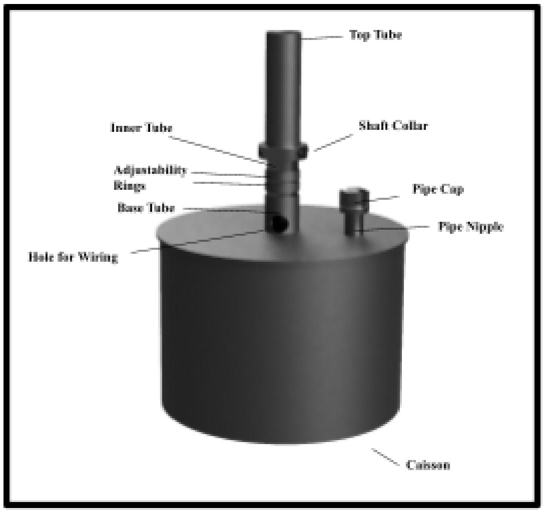

Figure 9: CAD of Caisson Foundation

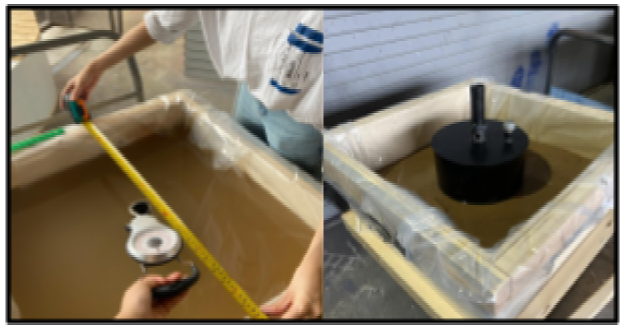

Figure 10: Foundation Testing

The outer tube is divided into outer sections that slide over an inner tube welded to the top plate. The 4 cm base tube is welded to the top plate, providing a clean edge for the 1 cm adjustability rings to sit on. Both the inner tube and the base tube have a hole for wires to exit. The adjustability rings can be added or removed to raise or lower the top tube to between 16-18 cm above the sand. To prevent the 12 cm top tube from rotating, a shaft collar welded to half of the bottom of it is tightened around the inner tube. The final weight of our foundation is around 8.8 lb_m.

All adjustability will be performed before installation, determined by measuring the height of the sand with respect to the top of the tank. The shaft collar around the top tube will be tightened above the correct number of adjustability rings. During installation, the pipe nipple allows fluid to exit. When the top of the caisson is resting on the sand, the hole in the top of the foundation piece is sealed by screwing on the pipe cape with our installation tool. Thus, the caisson creates a suction in response to any movement because no water or sand can fill the extra volume that would be created. This resistance to pressure change creates the suction that keeps the foundation anchored in the sand.

We built a wooden testing tank to competition dimensions to test our foundation by applying force with a luggage scale. The goal was to determine the force withstood before the foundation was displaced more than one inch. The minimum force required to move our foundation 1 inch was 289 N, which gives a moment applied to the foundation of 49.13 N-m. Based on our calculations, the maximum torque our foundation will be subjected to is 13.22 N-m. This gives us a factor of safety of 3.7.

2.6 Electrical Analysis and Electrical Diagram of Overall System

2.6.1 System Design Overview

The electrical system consists of three main sides: nacelle, turbine, and load. Figure 11 illustrates the layout of the circuit. The nacelle was designed to contain the most essential components such as the generator, linear actuators to control the pitch, and key sensors for data collection. The turbine side aims to convert the three-phase DC output of the generator into a usable DC form, and regulate the power to components in the nacelle. Then the produced power is sent through the emergency stop connected in series with the point of common coupling and then into the load. The Arduino Uno on the load side collects data from the nacelle side sensors and control switches used for restarting the turbine after shutdown.

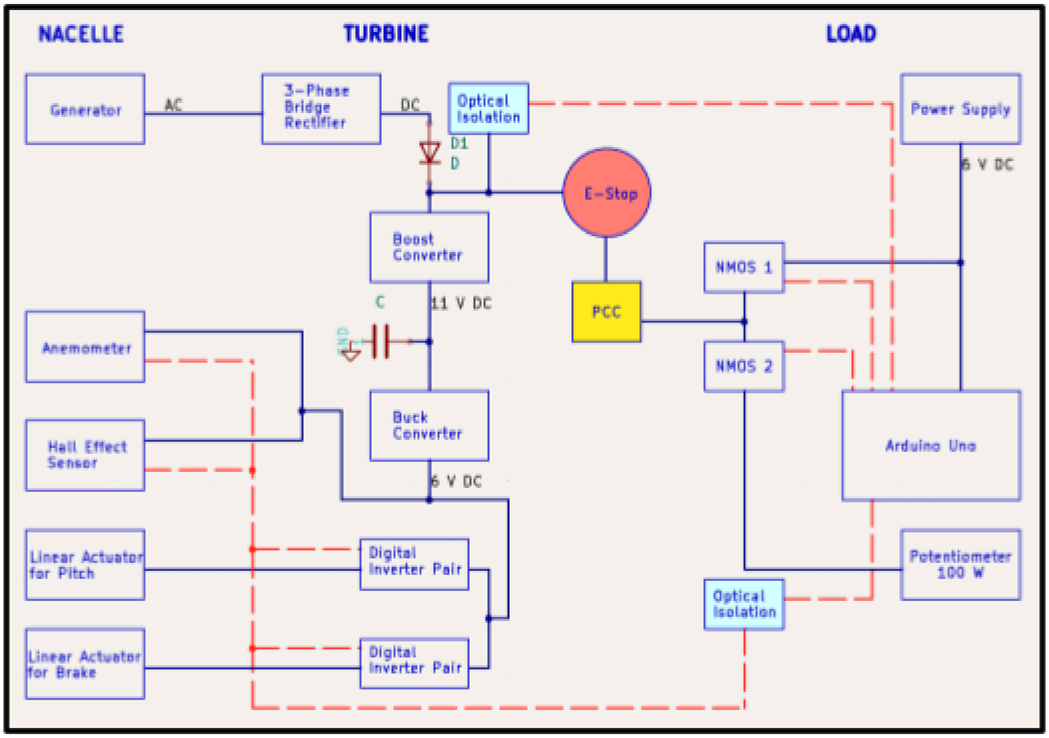

Figure 11: One-line Diagram of Overall Circuit
Power - Solid Navy Line
Communication - Dashed Red Line

2.6.2 Generator

Our design utilizes the Nanotec DB42C01 brushless 3-phase DC Motor which is rated for a power of 157 W, a current of 4.63 A, a voltage of 48 V, a speed of 6000 RPM, and a torque of 35.4 oz-inches. It has a peak torque specification of 106.21 oz-in and a peak current rating of 13.89 A. We considered the motor appropriate, considering safety regulations that the motor voltages be under 48 V and the fact that we remain well within the limits and tolerances of the motor when testing our turbine in a wind tunnel. We then successfully followed the generator with a custom-built three-phase bridge rectifier to convert the output to DC.

2.6.3 Buck-Boost Converter

We utilize a turbine side buck/boost converter system to regulate the various control signals used throughout our design. The output power from the turbine is first passed to the boost converter, where it is boosted to 11 Volts, a value large enough to surpass the threshold for our buck converter that follows the boost. This boosted voltage is then passed to a buck converter that bucks voltage down to 6 V to provide the correct functionality for downstream components such as the turn-on voltage for the anemometer, hall effect sensor, and linear actuators. Additionally, a 6.05 J, 11 V, and 0.1 F capacitor between the boost and buck converter stores energy during the regular functioning state and supplies power to the linear actuators to pitch out of the wind and turn on the disk brake during the emergency stop.

2.6.4 Anemometer and Hall Effect Sensor

The anemometer and hall effect sensor measure wind speed and RPM respectively. Both sensors have a turn-on voltage of 5V, supplied through the buck converter. These signals are then run through optocouplers before reaching the Arduino.

2.6.5 Power Optimization and Electrical Load

In an effort to determine an appropriate load for our turbine, we performed experiments with our generator and a variable load (potentiometer). By situating the generator in a lathe, we were able to set an RPM for it to spin our generator at. For many discrete RPM values tested, we connected a potentiometer load and swept through its range of resistances–1 to 10 ohms–and recorded the measured power. Our experiment found that the power our generator produced increased rapidly with RPM, and that the electrical load that resulted in the highest measured power for each RPM was consistently 3 ohms. As such, we concluded that with our current setup, an electrical load of 3 ohms was appropriate for optimizing our power output.

2.6.6 MOSFET System

To control the flow of power through our turbine, we employ MOSFET devices, particularly NMOS devices, to act as switches. NMOS devices are off by default, meaning they act as an open circuit, not allowing any power to pass through them until they receive the appropriate gate signal, a digital 1. This gate signal will come from our Arduino and is calculated based on the control states. We chose to use Nexperia's PSMN1R1-30PL NMOS for its relatively low Vgs of 1.3 V and high drain-source breakdown voltage of 30 V. This will allow us to open and close the NMOS with low voltages while it can withstand high voltages without damage.

1. Regular Functioning State: NMOS 1 is open while NMOS 2 is closed, letting current flow into the load.
2. Restart State: NMOS 1 is closed while NMOS 2 is open, allowing current from the battery to travel across the PCC and power the linear actuators to unbrake and pitch back into the wind.

2.6.7 Electrical System Layout

Our electrical system is currently housed on two separate breadboards (one for turbine side electronics and one for load side electronics) within independent sealed plastic enclosures. Communication signal wires and power transmission lines (22 AWG and 18 AWG respectively) are routed into and out of these two boxes through cable glands drilled into their sides.

2.7 Control Model Analysis of the Operational Modes

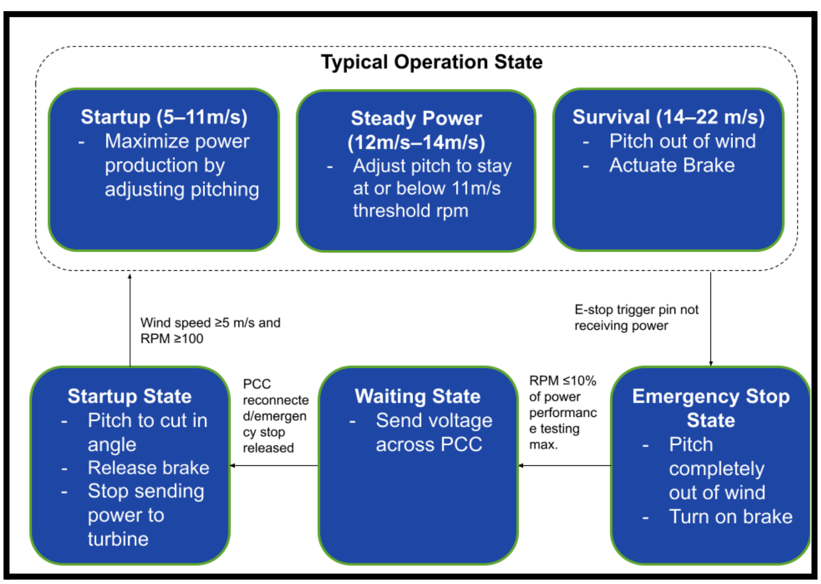

Figure 12. Operational Modes Flow Chart

Primary Operational Modes:
Startup: In the starting state of the turbine, the pitch to its cut in angle is set to allow the turbine to begin to spin at a low wind speed. Once the generator produces adequate voltage for the buck-boost converter system to provide 6 V to sensors, the Arduino receives data to adjust the pitch.
Emergency Shutdown: Emergency shutdown is initiated when the emergency stop button is pressed, which breaks the connection through the PCC. If the Arduino detects 0 W power output, a signal is sent to the digital inverter pairs which activate the linear actuators to completely pitch out of the wind and apply a disk brake.
Waiting State: Once the hall effect sensor stops receiving power and the Arduino reads the RPM as 0, it initiates sending power across the PCC to the turbine.
Restart: The system initiates restart when the turbine side circuit starts receiving power because the emergency stop button is released or the PCC is reconnected. Then, the system repeats the initial startup state.
Steady Power: To supply the load with constant power, it is imperative that RPM is regulated at the desired range. At wind speeds 12-14 m/s, we must adjust pitch to retain the RPM determined at 11 m/s wind speed. We do this by measuring the RPM and wind speed to record the RPM at 11 m/s wind speed and adjust the pitch to conserve that value when the wind speed is greater than 11 m/s.
Survival: For wind speeds exceeding 14 m/s, the linear actuators are activated such that the blades are pitched completely out of the wind and the disk brake is applied. A RPM close to 0 is desired to ensure the safety of the turbine.

2.8 Software Architecture and Development

The software was developed in small chunks to perform each task before being combined into the whole control structure. These sections included reading RPM, reading wind speed, power production, and controllability. The base of the RPM code was written with the help of generative AI in order to read RPM values based off of the readings of the hall effect sensor. The wind speed section was created using code provided by the anemometer manufacturer, Modern Devices, and adjusting the wind speed calibration curve in order to account for the effects of optical isolation. The code for power production and controllability was produced by the senior design team in charge of pitch development. Both sections made use of the Servo arduino library in order to control the linear actuator for pitching. Power production aims to maximize the RPM of the turbine by adjusting the pitch angle and comparing to previous RPM values until it finds the maximum. The controllability section sets a target RPM based off of our value at 11 m/s and utilizes proportional control in order to adjust the pitch and maintain that RPM.

These sections were then combined into the final code in accordance with the controls structure above. The code loops through continuously checking parameters such as RPM, wind speed, and whether power is flowing across the PCC. Furthermore, there is a flag system control which functions get triggered that keeps track of when the turbine is in emergency stop mode. This data is then used to trigger each control state and drive the turbine functionality.

2.9 Description of Final Wind Turbine Assembly

2.9.1 Description of the Final Assembly of Turbine Subsystems

The final assembly of the turbine starts with preparing the pitch system. The D-profile shaft is cut down to length and tapped with three holes to accommodate blade couplers. Once the shaft is prepared, brass pins attach each coupler to a leg and each leg to the upper swashplate. The upper swashplate prints in two pieces to accommodate a needle bearing. Once the needle bearing is on, epoxy is applied and the upper swashplate pieces key together. The hub is epoxied onto the shaft and needle bearings are installed. The upper swashplate then threads onto the shaft and the couplers are screwed into the tapped holes using shoulder screws. Then another needle bearing slides onto the shaft behind the upper swashplate along with the linear rotary bearing. The lower swashplate halves then go around the upper swashplate and halves are screwed together.

The nacelle assembly starts by press fitting two main bearings in the front section and securing a sleeve bearing in the neck with epoxy. The faceplate of the nacelle holds the main bearings in place and is screwed into heat set inserts in the front of the nacelle. The disc brake caliper is then screwed into the support inside the nacelle. The disc brake caliper transition piece is screwed onto the linear actuator and both actuators and the generator are put into the nacelle beds. As we install the electrical components, the wires slide down a cutout and out the neck. Then the shaft with the pitch system assembly slides through the main bearings, and we install a shaft coupler for spacing along with our disc and the main shaft coupling. The main coupling then clamps down on the main shaft and the motor shaft and the lower swashplate is secured to the linear actuator with a nut and bolt. The final step in nacelle assembly is to add the lid which has custom cutouts for all components in order to secure them fully. The lid has a rim to press fit onto the bottom of the nacelle and it is screwed down into heat set inserts for added security

During commissioning, JST connectors are used to connect to the wires from the electrical components in the nacelle to the main cable which is threaded through the turbine tower. The base plate is secured to the transition stub with M10 washers and bolts. The transition stub sits on the top tube of our foundation. The anemometer cable tightly spirals down the exterior of the tower, then clamped to the tower, with the face oriented perpendicular to the wind direction. The main cable comes out of our foundation and into the turbine side electrical box. Out of the electrical box are wires with JST connectors to connect to the load side electrical box. Also in between the electrical boxes is the required Anderson powerpole for the PCC connection. Lastly, the load side circuit box is connected to wall power via a 6 V 500 mA power brick.

The brass sleeve bearing in the nacelle is twisted on the tower to face the predominant wind direction. The shaft collar is then tightened to lock the yaw. Consequently, the only components that are adjusted during tunnel testing are the pitch system and the disk brake. The pitch system is adjusted by supplying power to the pitching linear actuator. The disk brake is utilized by actuating the braking linear actuator to close the brake calipers and press the pads against the aluminum disc brake.

2.9.2 Discussion of Managing a Distributed Team Environment

Our two subteams, Mechanical and Electrical, held weekly 2-hour meetings with 30 minutes of overlap between meetings to facilitate any necessary integration communication. One lead was appointed Chief Engineer to call integration meetings and facilitate logistical planning for testing. Every meeting began with updates followed by tasks to be done, with a lead assigned to each task as a point of contact. Members then had the choice of tasks laid out, and were always encouraged that lack of experience should not deter them from a task. Skills that both members and leads learned throughout include coding, circuit analysis, soldering, conducting power generation tests, machining on the mill and lathe, using the water jet cutter, 3D printing, using Fusion360 CAD, sizing and selecting components, and conducting static and vibration tests. Leads met for 30 minutes either before or after their team meeting to assess progress and plan the next meeting. As designing blades is a specialized and intricate task, all blade design was done in separate 1-hour meetings by a Mechanical team lead.

2.10 Assembly and Commissioning Checklist

Prior to commissioning, our systems will be tested after assembly at our team table to ensure functionality. These systems include pitch actuation, disc brake, hall effect sensor, and anemometer.

Commissioning (to be completed in 3 minutes)

- [ ] Thread main wires through the bottom of the tower
- [ ] Pull main wires to remove excess and slide the base plate on top of the transition stub mounting bolts
- [ ] Connect nacelle JST connectors to JST connectors on cables
- [ ] Connect turbine side and load side Anderson Powerpole connectors to PCC

- ☐ Connect from turbine side to load side the voltage output of the anemometer, hall effect sensor, and ground pin
- ☐ Secure each bolt with an M10 washer and wing nut
- ☐ Twist the nacelle on the sleeve bearing to face the predominant wind direction
- ☐ Tighten the shaft collar, positioned halfway across the sleeve bearing and the tower with the 3/16” allen key on the red set to lock the yaw
- ☐ Align the anemometer with the predominant wind direction
- ☐ Enact reset protocol in code (send 5V to pin 3)
- ☐ Visually verify that blades are at start-up pitch position
- ☐ Manually spin the blades to ensure the shaft is not obstructed and spins freely
- ☐ Tug on each blade coupler to ensure the shoulder screws are fully tightened
- ☐ Connect to wall power

2.11 Field Testing Analysis

We conducted field testing in wind tunnels at Rice and at Texas A&M University (TAMU). The Rice wind tunnel has a small cross section, so we used scaled down blades. Tests at Rice facilitated subsystem testing of the pitch system, disc brake, anemometer, and controls logic. The largest limitation is that we could not fit our tower or competition-sized blades, which we were able to test at TAMU.

2.11.1 Rice Wind Tunnel Testing Results

In testing at the Rice wind tunnel, we confirmed we were able to start and stop the turbine by pitching the blades, that our couplers and blades were strong enough up to 3,000 RPM, higher than our expected operating range. We identified that our main bearing had too much flex and would allow the shaft to rattle and that our pitch shoulder screws would loosen ¼ turn over time. We remedied this by adding two main bearings for stability and using loctite to secure the shoulder screws. We saw that our components were vibrating up and down in their nacelle mounts and the main bearing was not secure. We created a custom lid that molds over the nacelle components to stop them from vibrating, and changed the printing orientation of our nacelle so that the bearing mount would not need any supports. We also noticed that our braking disc was wearing down the bottom of our nacelle bed, and turned our discs down on a lathe to be smaller.

Further, we were able to calibrate the anemometer IC through optical isolation at various wind speeds and test the accuracy of our hall effect sensor RPM readings. We were also able to confirm the operation of the controls logic and our ability to pitch out of the wind for emergency stop using the energy stored in the capacitor.

2.11.2 Texas A&M University Wind Tunnel Testing Results

Our tests at TAMU allowed us to conduct testing with the final blades and tower. We have made two testing trips so far and will make one more prior to competition to conduct a mock testing trial.

At our first test, we controlled the pitch and disc brake actuators manually with wall power and limit switches. We were able to pitch the blades and cut in at 4.5 m/s, which proved our success in minimizing friction in the pitch system. With the blades fully feathered out of the wind, the rotor did not start spinning until 21 m/s. With our disc brake actuated, the rotor did not move in 22 m/s wind. We want to keep our rotor stationary to minimize the stress on the system and reduce the moment that the turbine exerts on the foundation. Based on our testing, we are confident that our turbine structure will pass the durability task.

Prior to this test, our nacelle neck cracked due to hoop stress, so we had to tape the nacelle to ensure it did not yaw about the sleeve bearing-nacelle connection during testing. This was due to the print orientation change made to better house the bearings after Rice wind tunnel testing. To remedy this, we separated the nacelle neck as a separate piece and reprinted it without layer lines vulnerable to hoop stress.

We hypothesized that remaining shaft wobbling was due to unbalanced blades. Our blade stubs were hand-sanded a few millimeters, so we modified our blade files to require no sanding of the stubs to fit in the couplers. This ensures the blades are as close to each other as possible and any human error in manufacturing is minimized.

Full system testing also allowed us to identify RPMs with turbulent vibrational resonant frequencies. The main mode we traverse through is at 1200. We have adjusted our code logic not to choose 1200 as an optimal operating RPM, but to instead traverse to 1400 which is smooth and stable.

At our next test, we integrated the pitch and disc brake actuators to be controlled by our Arduino. We experienced more difficulty with startup, and upon opening the nacelle lid discovered brake caliper dust because our disc was secured too close to the back caliper. Once remedied, we were able to test initial power performance included in Table 1 below. Data collection for power generation allowed us to confirm the results of our generator testing in which we found that power was optimized at ~3 Ohms load resistance.

Table 1: Performance Data from TAMU Testing

Wind Speed (m/s)	**Pitch (degrees)**	**RPM (rev/min)**	**Power (Watts)**
8	20	1100	3.4
9	10	1700	7.26
10	15	1700	7.35
11	20	2600	12.05

The team has had great success this year in prototype durability throughout all testing. Not a single component has been broken during testing, no blades have been broken, and no fasteners have come off or loosened to the detriment of our functionality. We have continued testing in the Rice wind tunnel, preparing for our mock competition trial at TAMU.

References

[1] Ragheb, Magdi, and Adam M. 'Wind Turbines Theory - The Betz Equation and Optimal Rotor Tip Speed Ratio'. Fundamental and Advanced Topics in Wind Power, InTech, 20 June 2011. Crossref, doi:10.5772/21398.

[2] Desalegn, Belachew, et al. "Onshore Versus Offshore Wind Power Trends And Recent Study Practices In Modeling Of Wind Turbines' Life-Cycle Impact Assessments." *Cleaner Engineering and Technology*, vol. 17, Nov. 2023, https://doi.org/10.1016/j.clet.2023.100691